

# Broad $H\alpha$ wings in Nebulae around Evolved Stars and in Young Planetary Nebulae

A. ARRIETA <sup>1</sup> AND S. TORRES-PEIMBERT

*Instituto de Astronomía (UNAM), Ap. Postal 70-264, México D.F. 04510 México*

`anabel@astrocu.unam.mx`

## ABSTRACT

Eleven objects that have been reported as proto-planetary nebula or as young planetary nebulae that show very extended  $H\alpha$  wings are presented. The extension of these wings is larger than  $800 \text{ km s}^{-1}$ . Data for two symbiotic stars that show this same characteristic is also presented. Raman scattering is the mechanism that best explains the wings in 10 of the PNe and in the 2 symbiotic stars. In the PN IRAS 20462+3416 the wing profile can be explained by very intense stellar wind.

*Subject headings:* ISM:planetary nebulae–binaries:symbiotic–scattering– stars:mass-loss–stars: AGB and post-AGB - Line: profiles

## 1. Introduction

As part of a study of proto-planetary nebulae and young planetary nebulae we have observed 59 objects that have been selected for fulfilling one or more of the following criteria: post-AGB stars with evidence of high mass loss rate, or PNe with low degree of ionization or with  $H_2$ , CO or OH molecular emission; all the objects observed have IRAS colors typical of planetary nebulae. In the sample, 13 objects were outstanding for exhibiting extremely broad  $H\alpha$  lines, of these, 10 have not been reported previously as having this characteristic. The  $H\alpha$  profiles selected for being extremely broadened are presented in this work.

Very wide  $H\alpha$  emission lines have been reported previously in other objects in the early stages of planetary nebulae phase; these include seven post-AGB stars, five young PNe and some symbiotic stars (Van de Steene, Wood & van Hoof 2000; Lee 2000; Lee & Hyung

---

<sup>1</sup>Present address: Space Telescope Science Institute

2000; Miranda, Torrelles & Eiroa 1996; Balick 1989; López & Meaburn 1983; Van Winckel, Duerbeck & Schwarz 1993; Wallerstein 1978). Lee & Hyung (2000) advanced the proposal that the broad wings are produced by Rayleigh-Raman scattering which involves atomic hydrogen, whereby Ly $\alpha$  photons with a velocity width of a few  $10^2 \text{ km s}^{-1}$  are converted to optical photons and fill the H $\alpha$  broad region. In the present work this mechanism is investigated further and alternate possibilities for H $\alpha$  broadening are examined.

## 2. Observations and reductions

The observations were carried out at the Observatorio Astronómico Nacional in San Pedro Mártir, Baja California with the 2.1-m telescope and the REOSC echelle spectrograph ( $R \sim 18,000$  at  $5,000 \text{ Å}$ ) and a  $1024 \times 1024$  Tektronix detector that yields a spectral resolution of  $10.6 \text{ km s}^{-1}$  and a spatial resolution of  $0.99''$  per pixel. The  $3600$  to  $6800 \text{ Å}$  range was covered in 29 orders. For extended objects the slit was centered on the nucleus. The observing log of those objects with wide H $\alpha$  wings is presented in Table 1.

The data reduction was carried out with IRAF routines using ‘echelle’ and ‘ccdred’ tasks. Calibrated spectra for most of the objects were obtained. The orders were extracted using a 10 pixel window. A HeAr lamp was used for wavelength calibration and the standard stars by Hamuy et al. (1992) were observed for the flux calibration.

In several cases the objects exhibit extremely wide H $\alpha$  lines, with full widths at zero intensity, FWZI, larger than  $800 \text{ km s}^{-1}$ . In order to ascertain whether the wide wings are real or due to instrumental effects the “number of counts at maximum” vs. FWZI both for the brightest unsaturated lines of the comparison lamp spectra and for H $\alpha$  emission lines in our sample were compared. Objects with FWZI  $> 1000 \text{ km s}^{-1}$  and those with significantly broader wings in H $\alpha$  than what can be considered instrumental were selected for this study; namely, those with FWZI  $3\sigma$  above the observed ones for comparable line intensities in the HeAr lamp.

## 3. H $\alpha$ wings

The H $\alpha$  profiles for the 13 selected objects are shown on Figure 1. To better visualize the line profiles, an enlargement along the intensity to display the wings over the full H $\alpha$  profile is presented. In all cases the FWZI is significantly larger than expected from a gaussian fit to the core of the profile. No correlation between the line intensity and the width of the wings was found.

The main spectral characteristics of each object are presented in Table ?? . It includes the ions present in emission and absorption in our spectra and the stellar spectral type (as taken from SIMBAD database). For the 13 objects  $H\alpha$  FWZI and  $H\beta$  FWZI where it is significantly larger than expected from a gaussian fit to the core of the profile are presented in Table 3. In this table the most common classification in the literature for each object, nebular morphology, possible binarity and type of  $H\alpha$  line profile are included.

## 4. Possible mechanisms for wing broadening

### 4.1. Rotating disks

For this case maximum velocity would correspond to the circular velocities at the surface of the exciting star,

$$v_{max} = 437 \sqrt{(m/M_{\odot})/(r/R_{\odot})} \text{ km s}^{-1} ,$$

which for young PNe central stars of  $m = 0.6 - 0.83 M_{\odot}$ , and  $r = 1 - 18 R_{\odot}$  would correspond to  $v_{max} < 400 \text{ km s}^{-1}$ , although for symbiotic stars, where the hot component is small  $r < 0.1 R_{\odot}$ , larger velocities could be achieved. Nevertheless, for both PNe and symbiotic stars,  $v_{max}$  is not large enough to explain the observed broadening which reaches up to  $5000 \text{ km s}^{-1}$  in some cases. Thus the possibility that in PNe emission from a rotating disk would explain by itself the extended wings can be ruled out.

### 4.2. Stellar winds

The possibility for the line wings to be formed in the region dominated by stellar winds was tested by examining the existing IUE spectra for each object looking for evidence of P Cyg profiles in resonant lines of ions like C IV, C III, He II, Al III, Mg II and Si IV.

Only one object (IRAS 20462+3416) shows P Cyg profile evidence both in our optical spectra and in the UV. Furthermore, IRAS 20462+3416 shows an anomalous broadened emission in  $H\alpha$ , that is  $+110 \text{ km s}^{-1}$  from the narrow emission line. This profile shows significant deviations from the  $\Delta\lambda^{-2}$  profile that can be fit to the other broad wings (see Figure 1). The presence of P Cyg profiles both in optical and UV spectra, and the  $H\alpha$  wing profile suggests that stellar wind is the mechanism that is producing these features. In a separate paper (Arrieta, Torres-Peimbert, Georgiev & Koenigsberger 2003) it is shown that indeed the  $H\alpha$  profile of this object can be explained by a very strong stellar wind. The  $H\alpha$  profiles for the rest of the objects cannot be explained with stellar winds.

### 4.3. Electron scattering

This mechanism has been proposed, and has been intensively studied, as the line broadening mechanism in QSOs (e.g. Mathis 1970; Shields & McKee 1981; Lee 1999) and in WRs (e.g. Hillier 1991). Given that the cross section of electron scattering is independent of wavelength it is to be expected that other intense emission lines formed in the same region as  $H\alpha$  are similarly broad.

Extended wings in other bright emission lines of our optical spectra were searched for. No broad extensions in forbidden lines in any of the objects were found. The objects IRC+10420, M 1-92, HM Sge, M 3-60, and Z And showed extended wings in  $H\beta$ . In all cases the width of  $H\beta$  is significantly smaller than that of  $H\alpha$  (see Table 3). It is possible that in the other objects the low signal-to-noise ratio masks the low intensity extended wings. For objects with broad  $H\beta$  wings no correlations were found with the presence of the  $H\beta$  wings and the width of  $H\alpha$ , nor with the  $H\alpha/H\beta$  line ratios.

The necessary conditions for the  $H\alpha$  wings to be produced by electron scattering were investigated. Given that no significant broadening was found in the forbidden lines, it is required for the forbidden line region to be exterior to the electron scattering region. A two-region geometry was assumed: (a) a recombination line emitting region where a substantial fraction of  $H\alpha$  is produced, dense enough to suppress the forbidden lines, and where most of the scattering takes place ( $N_e > 10^6$ ,  $T_e \sim 10^4$ ) (b) and an external low density forbidden line emitting region ( $N_e = 10^4 - 10^6 \text{ cm}^{-3}$ ,  $T_e \sim 10^4$ ). It is also possible to consider that region (a) consists of a point source where most of the  $H\alpha$  is produced surrounded by a dense scattering region.

To derive the temperature in the electron scattering region from the observed  $H\alpha$  line profiles the treatment proposed by Mathis (1970) was followed. The main parameter is the width of the wings, defined as  $Y(2) \equiv F_{obs}(\Delta v_M)/F_{obs}(2\Delta v_M)$ , which essentially determines the temperature of the electron scattering region,  $T_{ES}$ . The optical depth of the scattering region,  $\tau_{ES}$ , can be derived from the ratio of the strength of the unscattered core of the line relative to its total strength  $w \equiv F(unscattered)/F(total)$ , which determines the optical depth of the scattering region,  $\tau_{ES}$  (Osterbrock 1980). For the simple case of a spherically symmetric scattering region of uniform density and temperature for the case of M2-9  $Y(2) = 2.05$ , and  $w = 0.83$  can be obtained. From these values a temperature,  $T_e \sim 10^8 \text{ K}$ , and optical depth,  $\tau_{ES} \sim 0.24$  can be found, the latter coupled to a limiting size of  $r_{ES} < 10^{12} \text{ cm}$ , given by an unresolved central core of  $2''$ , yields a density  $N_e > 10^{12} \text{ cm}^{-3}$  for the electron-scattering region. From the values derived for M 2-9, which is representative of the whole sample, it was considered unlikely for this configuration to be the general case surrounding an AGB star and thus to account for the extremely wide  $H\alpha$  lines observed in

young PNe.

#### 4.4. Raman Scattering

Raman scattering describes the absorption of a photon, followed by the immediate re-emission of another photon at different wavelength where the intermediate state does not correspond to a true bound state of the atom. Initially this process was suggested by Schmid (1989) as the mechanism of production of the broad emission features at  $\lambda\lambda 6830$  and  $7088\text{\AA}$  found in 50% of symbiotic stars; he suggested that the emission features are due to Raman scattering of the O VI resonance doublet  $\lambda\lambda 1032$  and  $1038\text{\AA}$  by neutral hydrogen. Nussbaumer, Schmid & Vogel (1989) proposed a list of uv lines of different ions (including S III, He II, O I, O VI and C II), with wavelengths close to  $\text{Ly}\beta$ , as candidates for Raman scattering on the ground state of neutral hydrogen; these Raman scattered lines would be expected to be found in the  $6000 - 7000\text{\AA}$  , range. They noted the possibility that Raman scattering may also hold a clue to the broad line wings of  $\text{H}\alpha$ , occasionally observed in Seyfert galaxies and symbiotic stars.

Several of the emission features at different wavelengths that can be attributed to Raman scattering have been identified in symbiotic stars and in planetary nebulae. In symbiotic stars the identifications include, among others:  $\lambda\lambda 6830$ ,  $7088\text{\AA}$  from O VI  $\lambda\lambda 1032\text{\AA}$  and  $\lambda\lambda 7021$ ,  $7052\text{\AA}$  from C II  $\lambda\lambda 1036$ ,  $1037\text{\AA}$  in V1016 Cyg (Schmid 1989; Schild & Schmid 1996) as well as  $\lambda 4850\text{\AA}$  from He II (2-8)  $\lambda 972.1\text{\AA}$ ,  $\lambda 4331\text{\AA}$  from He II (2-10)  $\lambda 949.3\text{\AA}$ , and  $\lambda 4975\text{\AA}$  from C III  $\lambda 977.0\text{\AA}$  in RR Tel (van Groningen 1993). In planetary nebulae, they include  $\lambda 4850\text{\AA}$  in NGC 7027 (Péquignot et al. 1997), and  $\lambda 6545\text{\AA}$  from He II (2-6)  $\lambda 1025\text{\AA}$  in M2-9 (Lee et al. 2001).

Lee & Hyung (2000) proposed that the broad  $\text{H}\alpha$  wings of the PN IC 4997 are formed through Raman scattering that involves atomic hydrogen and, by which  $\text{Ly}\beta$  photons with a velocity width of a few  $10^2 \text{ km s}^{-1}$  are converted to optical photons and fill the  $\text{H}\alpha$  broad wing region. Their model fits the observations on the blue wing from  $v = 500$  to  $1500 \text{ km s}^{-1}$ , it requires relatively strong incident  $\text{Ly}\beta$  flux from an unresolved core of high density ( $N \sim 10^9 - 10^{10} \text{ cm}^{-3}$ ) and a column density for the scattering region of  $n_{\text{H}\alpha} = 2 - 4 \times 10^{20} \text{ cm}^{-2}$ . Lee (2000) further proposed that the  $\text{H}\alpha$  wings seen in symbiotic stars can be fit to Raman scattered profiles. For the optically thin case, where almost all the  $\text{Ly}\beta$  photons are scattered not more than once and assuming a flat incident  $\text{Ly}\beta$  profile, to the first order the wing profile can be approximated by a curve proportional to  $f(\Delta v) = \Delta v^{-2}$ . Lee adjusted this curve to  $\text{H}\alpha$  profile observations from  $200$  to  $1000 \text{ km s}^{-1}$  from the line center for 16 symbiotic stars.

Figure 1 shows the fit of curves proportional to  $\Delta v^{-2}$  to the wings of the 13 objects under consideration in this paper. In general the fits are satisfactory for 12 objects, excepting IRAS 20462+3416 where it does not at all fit the observed profile; the curves match the observations starting at 200 - 300  $\text{km s}^{-1}$  from the center of the line, to the outermost regions where the signal becomes too faint to be significant, this extreme velocity reaches up to 500 - 1500  $\text{km s}^{-1}$ . The differences in some objects can be explained in terms of non uniform motions in the ionized regions. The kinematics of these cases will be analyzed in later studies. In particular, CRL 618 and HM Sge show wider cores than the expected profile, while IRC+10420 shows a narrower core; M1-92 shows significant differences in the 300 - 800  $\text{km s}^{-1}$  region, which have been interpreted as a jet of material along the line of sight (Arrieta, Torres-Peimbert, & Georgiev 2000). The case of IRAS 20462+3416 is clearly different, because it does not fit at all such a  $f(\Delta v) = \Delta v^{-2}$  profile, neither in the core, nor in the wings. As mentioned in the previous section the interpretation of this profile corresponds to a very large mass loss rate (Arrieta, Torres-Peimbert, Georgiev & Koenigsberger 2003) .

The width required for  $\text{Ly}\beta$  emission to be responsible for the  $\text{H}\alpha$  wings has been investigated in more detail. Since the width of the scattered  $\text{H}\alpha$  is proportional to the initial width of the  $\text{Ly}\beta$  line, then,  $\Delta v_{\text{Ly}\beta} = \Delta v_{\text{H}\alpha}/6.4$  is expected. An estimate of the  $\text{Ly}\beta$  width can be given by other UV emission lines widths. A search in the UV high resolution spectra of MAST (Multimission Archive at Space Telescope) was carried out for the objects under consideration where data for Z And, HM Sge and IC 4997 were found. In the cases of Z And and HM Sge the Si III]  $\lambda 1892\text{\AA}$  line has width of  $\sim 500 \text{ km s}^{-1}$ , consistent with the  $\Delta v_{\text{Ly}\beta}$  width ( $\sim 625$  and  $\sim 468 \text{ km s}^{-1}$ ) required to produce the observed broadened  $\text{H}\alpha$  lines (as given in Table 3). In the case of IC 4997 the width of the Si III]  $\lambda 1892\text{\AA}$  line is of only  $\sim 160 \text{ km s}^{-1}$ . Although Lee et al. (2001) consider that since the  $\text{Ly}\beta$  underlying continuum emission is not likely to show a flat profile, it may be more plausible that the broad  $\text{H}\alpha$  wings are formed by Raman scattering of the continuum photons around  $\text{Ly}\beta$ .

Evidence of additional Raman scattered features in our optical spectra was searched for. The  $\lambda 6830\text{\AA}$  feature was found to be present in Z And and weakly in HM Sge with a FWZI  $\sim 1500 \text{ km s}^{-1}$  (this feature has been studied previously by Birriel et al. 1998; Schmid et al. 2000). Features around this wavelength were found in M 2-9, IRAS 17395-0841, IRC+10420, M 3-60, IC 4997 and possibly in M 1-92 with FWZI around a few  $10^2 \text{ km s}^{-1}$  and not a few  $10^3 \text{ km s}^{-1}$  as is the case in symbiotic stars. The  $\lambda 6545\text{\AA}$  feature in M 2-9 and M 1-92 as well as  $\lambda 4851\text{\AA}$  in IC 4997 with FWZI around few  $10^2$  of  $\text{km s}^{-1}$  were also found. In that same sense, the  $\text{H}\beta$  wings found in IRC+10420, M 1-91, HM Sge, M3-60, Hb 12 and Z And (see Table 3) can be explained by Raman scattering of the  $\text{Ly}\gamma$  line by the neutral hydrogen component.

In order to obtain additional indicators of the presence of neutral or molecular material along the line of sight a search in the literature was carried out for data on 21-cm measurements and the column density of atomic hydrogen. Only in the symbiotic star HM Sge and the planetary nebula IC 4997 21-cm column densities have been measured; in both cases values of  $n_{H^0} \sim 4 \times 10^{20} \text{ cm}^{-2}$  were determined. Also, following Dinerstein et al. (1995), evidence of nebular Na I doublet  $\lambda\lambda 5889, 5895\text{\AA}$  from our optical spectra was looked for, where Na I nebular components in 11 of our 13 objects were found; those with bright optical continuum and favorable radial velocities, (objects with radial velocities well separated from those expected for the interstellar material) which allow the separation of the nebular component and the narrow interstellar one. In addition a search in the literature for CO rotational transitions in radio wavelengths, roto-vibrational ones in the near infrared and H<sub>2</sub> roto-vibrational transitions was performed. The results are given in Table 4 where evidence of a neutral component at least in one of the indicators is listed.

## 5. Discussion and summary

We confirm that Raman scattering is the most probable mechanism for the formation of the H $\alpha$  broad wings in 12 of the 13 objects under consideration. This is supported by a fit of the profile to a  $\Delta v^{-2}$  law, by the presence of Raman produced features in emission, and by additional indicators of the presence of a significant neutral hydrogen component.

Evidence of neutral components in other 29 objects observed with H $\alpha$  in emission was searched for, in order to compare with the sample presented here. However there was not enough information in the literature to derive significant statistical data between the objects that show extreme wing widening and those that do not show it. Only in the case of the hydrogen molecule it was found that those objects with broad H $\alpha$  wings have H<sub>2</sub>, while those that are not broadened, do not.

Most of the objects with broad lines seem to have common characteristics: bipolar morphology, and composite emission line profiles, furthermore, they are compact objects in the process of forming a planetary nebula and very probably they are sites of wind interaction.

More detailed studies of the conditions for Raman scattering to take place and thus for the presence of surrounding neutral hydrogen could give us information about the processes that take place in giving rise to bipolar planetary nebulae.

We are grateful to M. Bautista, L. Georgiev y E. Villaver for fruitful discussions and to H. M. Schmid for many important suggestions to the original manuscript. Support from

DGAPA-IN100799, DGAPA-IN114601 and CONACyT-25451E grants is acknowledged.

## REFERENCES

- Alcolea, J., Bujarrabal, V., Castro-Carrizo, A., Sánchez-Contreras, C., Neri, R., & Zweigle, J. 2000, in *Asymmetrical Planetary Nebulae II: From Origins to Microstructures*, ASP Conference Series, Vol. 199. eds. J.H.Kastner, N.Soker & S.Rappaport, p. 347
- Arrieta, A., Torres-Peimbert, S., & Georgiev, L. 2003, to be submitted.
- Arrieta, A., Torres-Peimbert, S., Georgiev, L. & Koenigsberger, G. 2003, to be submitted.
- Balick, B. 1989, *AJ*, 97, 476
- Birriel, J. J., Espey, B. R. & Schulte-Ladbeck, R. E. 1998, *ApJ*, 507, L75
- Neri, R. 1998, *ApJ*, 504, 915
- Dinerstein, H. L., Sneden, C. & Uglum, J. 1995, *ApJ*, 447, 262
- Feibelman, W.A., & Bruhweiler, F.C. 1990, *ApJ*, 354, 262
- Hamuy, M., Walker, A. R., Suntzeff, N. B., Gigoux, P., Heathcote, S. R. & Phillips, M. M. (1992), *PASP*, 104, 533
- Hillier, D. J. 1991, *A&A*, 247, 455
- Hora, J. L., Latter, W. B. & Deutsch, L. K. 1999, *ApJS*, 124, 195
- Hrivnak, B. J., Kwok, S., & Volk, K. M. 1989, *ApJ*, 346, 265
- Huggins, P. J. & Healy, A. P. 1989, *ApJ*, 346, 201
- Josselin, E., Bachiller, R., Manchado, A. & Guerrero, M. A. 2000, *A&A*, 353, 363
- Kastner, J. H., Weintraub, D. A., Gatley, I., Merrill, K. M. & Probst, R. G. 1996, *ApJ*, 462, 777
- Knapp, G. R. & Morris, M. 1985, *ApJ*, 292, 640
- Kwok, S. 1982, *ApJ*, 258, 280
- Leahy, D. A., Taylor, A. R. & Young G. 1990, *AJ*, 99, 1926
- Lee, H.-W. 1999, *ApJ*, 511, L13
- Lee, H.-W. 2000, *ApJ*, 541, L25
- Lee, H.-W. & Hyung, S. 2000, *ApJ*, 530, L49

- Lee, H.-W. Kang, Y. -W. & Byun, Y. -I. 2001, ApJ, 551, L121
- López, J. A. & Meaburn, J. 1983, MNRAS, 204, 203
- Mathis, J. S. 1970, ApJ, 162, 761
- Mikolajewska, J. & Kenyon, S. J. 1996, AJ, 112, 1659
- Miranda, L. F., Torrelles, J. M. & Eiroa, C. 1996, ApJ, 461, L111
- Mueller, B. E. A. & Nussbaumer, H. 1985, A&A, 145, 144
- Nussbaumer, H., Schmid, H. M. & Vogel, M. 1989, A&A, 211, L27
- Osterbrock, D.E. 1989, in *Astrophysics of Gaseous Nebulae and Active Galactic Nuclei*, (San Francisco: Freeman), p.80
- Péquignot, D., Baluteau, J. -P., Morisset, C. & Boisson, C. 1997, A&A, 323, 217
- Rodríguez, M., Corradi, R. L. M., & Mampaso, A. 2001, A&A, 377, 1042
- Schild, H. & Schmid, H. M. 1996, A&A, 310, 211
- Schmid, H. M. 1989, A&A, 211, L31
- Schmid, H. M., Corradi, R., Krautter, J. & Schild, H. 2000, A&A, 355, 261
- Schwarz, H. E., Aspin C., Corradi, R. L. M., & Reipurth, B. 1997, A&A, 319, 267
- Shields, G. A. & McKee, C. F. 1981, ApJ, 246, L57
- Taranova, O. G., & Yudin, B. F. 1983, A&A, 117, 209
- Van de Steene G. C., Wood, P. R. & van Hoof, P. A. M., 2000, in *Asymmetrical Planetary Nebulae II: From Origins to Microstructures*, ASP Conference Series, Vol. 199. Ed. J. H. Kastner, N. Soker, & S. Rappaport
- van Groningen, E. 1993, MNRAS, 264, 975
- Van Winckel, H., Duerbeck, H. W., & Schwarz, H. 1993 A&AS, 102, 401
- Wallerstein, G. W. 1978, PASP, 90, 36

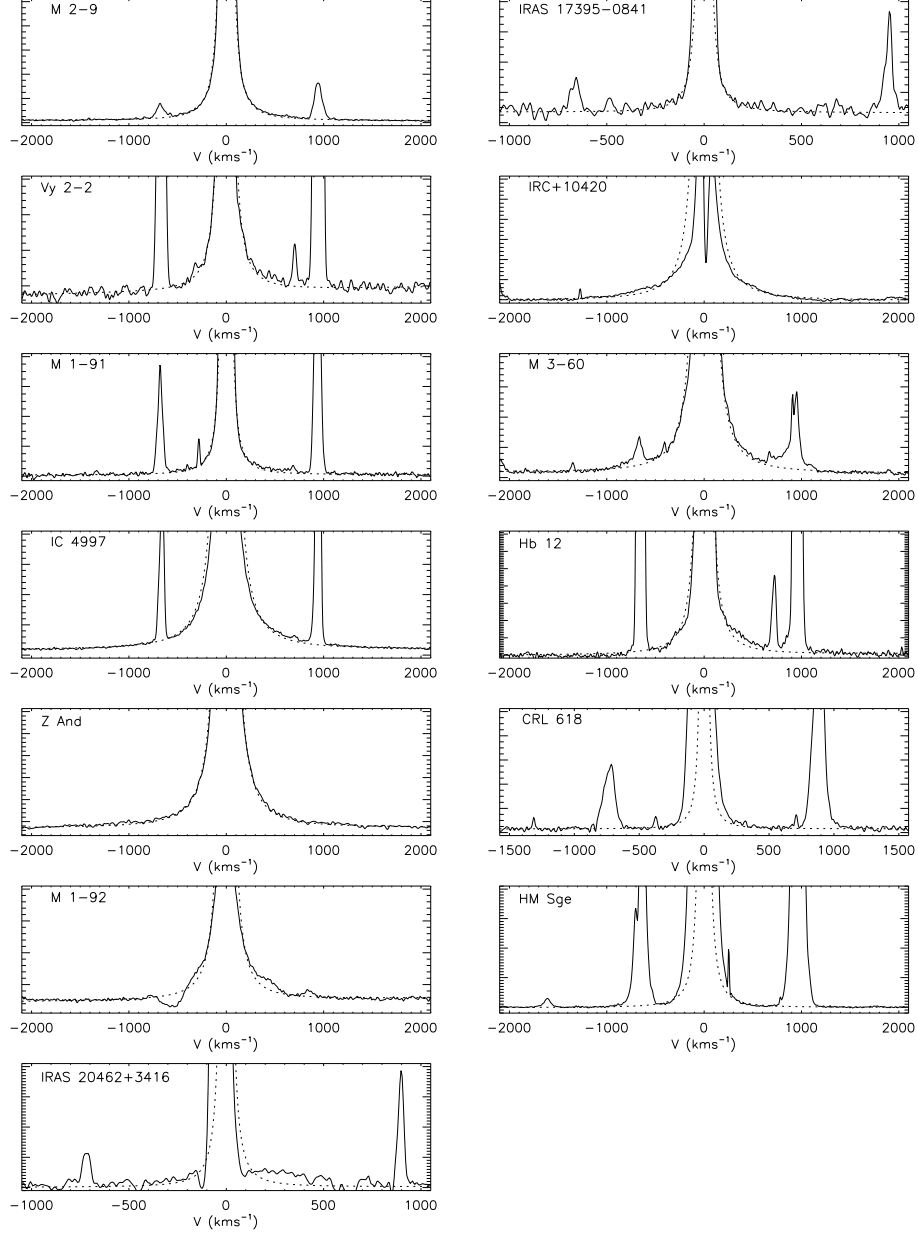


Fig. 1.—  $H\alpha$  profiles for the 13 selected objects of extreme broadening. In 12 cases a section of the spectrum between  $-2000$  and  $+2000$   $\text{km s}^{-1}$  is shown, and in one case  $-1000$  and  $+1000$   $\text{km s}^{-1}$ . Superposed to the observations is the  $1/v^2$  function that best adjusts to the wing profiles within  $\pm 100$   $\text{km s}^{-1}$  of the core.

Table 1: Observing log of objects with extended wings

Object	PNG	date observed	exposure time (sec)
CRL 618	166.4-06.5	5 Sep 95	1800
M 2-9	010.8+18.0	23 Apr 96	600
IRAS 17395-0841	017.0+11.1	10 Jun 97	1500
Vy 2-2	045.4-02.7	3 Jun 97	900
IRC+10420	-	27 Sep 95	900
M 1-91	061.3+03.6	11 Jun 97	2700
M 1-92	-	10 Jun 97	300
HM Sge	-	23 Apr 96	600
M 3-60	-	27 Sep 95	900
IC 4997	058.3-10.9	9 Jun 97	180
IRAS 20462+3416	-	6 Sep 97	1600
Hb 12	111.8-02.8	1 Sep 97	600
Z And	-	25 Sep 95	900

Table 2. Nebular and stellar spectral characteristics of the objects with very extended H $\alpha$  Wings.

Object	Emission lines	Absorption lines	Sp. type
CRL 618	H I, [Fe II], [N II], [O I], [O III], [S II]	non detectable	B0
M 2-9	H I, He I, He II, [Ar III], [Cr II], [Fe I], [Fe II], [Fe III], [Fe IV], [N II], [Ni II], [Ni III], [Ni IV], [O I], [O II], [O III], [S I], [S II], Si II	non detectable	Be
IRAS 17395-0841	H I, He I, [N II], [Ne III], [O I], [O III], [S II]	non detectable	–
Vy 2-2	H I, He II, [Ar III], [N II], [Ne III], [O I], [O II], [O III], [S II], [S III]	non detectable	Of
IRC 10420	H I, Cr II, Fe I, Fe II, Mg I, Sc II, Sr II, Ti II	H I, Ca II, Cr II, Fe I, Fe II, Na I, Si II, Ti II	F8 Ia
M1-91	H I, He I, [Fe II], [N II], [O I], [O III], [S II], [S III]	non detectable	Be
M 1-92	H I, He I, [Ca II], [Cr II], [Fe II], [N I], [N II], [O I], [O III], [S II], Ti II	H I, Ca II, Fe II, He I, N I	B0.5IV
HM Sge	H I, He I, He II, [Ar IV], C II, C III, [Fe II], [Fe III], [Fe IV], [Fe V], [Fe VII], [K IV], Mg I, [N II], N III, Ne II, [Ne III], O I, O II, O III, [S II], [S III], Si II	non detectable	M
M 3-60	H I, Fe II, [N II], [O I], [S II]	non detectable	B
IC 4997	H I, He I, [Fe II], [N II], [O I], [O III], [S II]	non detectable	
IRAS 20462+3416	H I, [N II], [S II], Si II	H I, He I, He II, Al III, Ca II, N II, Ne I, O II, S II, Si II	B
Hb 12	H I, He I, He II, Ar IV, C II, Cl II, Cl III, [Fe II], [Fe III], Mg I, [N II], N III, [Ne III], [O I], [O II], [O III], [S II], [S III], Si II, Si III	non detectable	–
Z And	H I, He I, He II, [Cr I], Fe II, [Fe VII], [K V], [Mn II], [O I], Si II	TiO	M6.5

Table 3: Characteristics of the objects with very wide H $\alpha$  wings (classification, morphology, binarity, profile type and widths of H $\alpha$  and H $\beta$ ).

Object	Classif.	Morphology	Binarity	Profile	H $\alpha$	H $\beta$
					FWZI (km s <sup>-1</sup> )	FWZI (km s <sup>-1</sup> )
CRL 618	Proto-PN	bipolar	-	double	2300	-
M 2-9	YPN	bipolar	probable (1)	double	5000	-
IRAS 17395-0841	Proto-PN	non resolved	-	simple	800	-
Vy 2-2	YPN	bipolar	-	simple	1400	-
IRC+10420	OH/IR	bipolar	no (2)	comp.	2600	1750
M 1-91	YPN	bipolar	probable (3)	double	1100	-
M 1-92	YPN	bipolar	yes (4)	double	2900	600
HM Sge	ymb.	bipolar	yes (5)	double	3000	1300
M 3-60	YPN	non resolved	-	double	2400	800
IC 4997	YPN	bipolar	-	double	5100	-
IRAS 20462+3416	YPN	oblate	-	PCyg	2200	-
Hb 12	YPN	bipolar	-	simple	1800	-
Z And	ymb.	non resolved	yes (6)	double	4000	1000

---

References. — (1) Schwarz et al. 1997; (2) Hrivnak et al. 1989; (3) Rodríguez et al. 2001; (4) Feibelman & Bruhweiler 1990; (5) Taranova & Yudin 1983; (6) Mikolajewska & Kenyon 1996

Table 4: Evidence of neutral components along the line of sight of those objects with wide H $\alpha$  lines.

Object	H I ( $10^{20}\text{cm}^{-2}$ )	Na I	H <sub>2</sub>	CO
CRL 618	-	yes	yes (3)	yes (5)
M 2-9	-	yes	yes (3)	yes (5)
IRAS 17395-0841	-	yes	-	-
Vy 2-2	-	yes (2)	yes (3)	no (5)
IRC+10420	-	yes	-	yes (6)
M 1-91	-	no	yes (4)	no (7)
M 1-92	-	yes	yes (3)	yes (8)
HM Sge	4 (1)	no	-	yes (9)
M 3-60	-	yes	-	-
IC 4997	3.8 (2)	yes (2)	no (4)	no (5)
IRAS 20462+3416	-	yes	-	-
Hb 12	-	yes	yes (3)	no (2)
Z And	-	yes	-	-

---

References. — (1) Leahy et al. 1990; (2) Dinerstein et al. 1995; (3) Hora et al. 1999; (4) Kastner et al. 1996; (5) Huggins & Healy 1989; (6) Knapp & Morris 1985; (7) Josselin et al. 2000; (8) Alcolea et al. 2000; (9) Mueller & Nussbaumer 1985.